Using noble gas tracers to constrain a groundwater flow model with recharge elevations: A novel approach for mountainous terrain

Jessica M. Doyle, Tom Gleeson, Andrew H. Manning, and K. Ulrich Mayer

October 2015

AGU PUBLICATIONS

Water Resources Research

RESEARCH ARTICLE
10.1002/2015WR017274

Key Points:
- Noble-gas-derived recharge elevation is used as calibration tool
- Recharge elevations can reduce model nonuniqueness
- Hydraulic head data alone are incapable of quantifying mountain block recharge

Correspondence to:
T. Gleeson,
tgleeson@uvic.ca

Citation:
Doyle, J. M., T. Gleeson, A. H. Manning, and K. U. Mayer (2015), Using noble gas tracers to constrain a groundwater flow model with recharge elevations: A novel approach for mountainous terrain, *Water Resour. Res.*, *51*, 8094–8113, doi:10.1002/2015WR017274.

Received 25 MAR 2015
Accepted 12 SEP 2015
Accepted article online 16 SEP 2015
Published online 12 OCT 2015

Using noble gas tracers to constrain a groundwater flow model with recharge elevations: A novel approach for mountainous terrain

Jessica M. Doyle[1,2], Tom Gleeson[3,4], Andrew H. Manning[5], and K. Ulrich Mayer[1]

[1]Department of Earth and Ocean Science, University of British Columbia, Vancouver, British Columbia, Canada, [2]Waterline Resources Inc., Nanaimo, British Columbia, Canada, [3]Department of Civil Engineering, McGill University, Montreal, Quebec, Canada, [4]Department of Civil Engineering, University of Victoria, Victoria, Canada, [5]U.S. Geological Survey, Denver, Colorado, USA

Abstract Environmental tracers provide information on groundwater age, recharge conditions, and flow processes which can be helpful for evaluating groundwater sustainability and vulnerability. Dissolved noble gas data have proven particularly useful in mountainous terrain because they can be used to determine recharge elevation. However, tracer-derived recharge elevations have not been utilized as calibration targets for numerical groundwater flow models. Herein, we constrain and calibrate a regional groundwater flow model with noble-gas-derived recharge elevations for the first time. Tritium and noble gas tracer results improved the site conceptual model by identifying a previously uncertain contribution of mountain block recharge from the Coast Mountains to an alluvial coastal aquifer in humid southwestern British Columbia. The revised conceptual model was integrated into a three-dimensional numerical groundwater flow model and calibrated to hydraulic head data in addition to recharge elevations estimated from noble gas recharge temperatures. Recharge elevations proved to be imperative for constraining hydraulic conductivity, recharge location, and bedrock geometry, and thus minimizing model nonuniqueness. Results indicate that 45% of recharge to the aquifer is mountain block recharge. A similar match between measured and modeled heads was achieved in a second numerical model that excludes the mountain block (no mountain block recharge), demonstrating that hydraulic head data alone are incapable of quantifying mountain block recharge. This result has significant implications for understanding and managing source water protection in recharge areas, potential effects of climate change, the overall water budget, and ultimately ensuring groundwater sustainability.

1. Introduction

Quantifying groundwater age, recharge, and flow characteristics is critical for evaluating aquifer sustainability and vulnerability [*Sanford*, 2002; *Scanlon et al*., 2002; *Senthilkumar and Elango*, 2004; *Gleeson et al*., 2010]. Quantifying groundwater flow is especially difficult in basin-fill aquifers in mountainous terrain, where subsurface inflow from adjacent mountain blocks (mountain block recharge) is a potentially large, yet often uncertain, recharge component [*Anderson et al*., 1992; *Wilson and Guan*, 2004; *Manning and Solomon*, 2005; *Manning*, 2011]. Mountain block recharge has primarily been recognized within alluvial basins located in semiarid climates, where mountain precipitation occurs mainly as snow and substantially exceeds precipitation on the basin floor [*Manning and Solomon*, 2003, 2005; *Magruder et al*., 2009; *Smerdon et al*., 2009; *Ajami et al*., 2011; *Manning*, 2011].

Environmental tracers in groundwater can be used to quantify groundwater age and characterize aquifer recharge and flow processes [*Cook and Bohlke*, 2000; *Plummer*, 2005]. This information, when combined with other hydraulic data, is valuable for evaluating and improving conceptual hydrogeological models. Tracers can be particularly useful for characterizing groundwater flow in mountain systems, where groundwater flow through fractured bedrock is complex and hydraulic data are often limited due to the difficulty and expense of drilling wells [*Wilson and Guan*, 2004; *Manning and Solomon*, 2005].

Environmental tracers can also provide additional, nontraditional or "unconventional" calibration targets in numerical groundwater models [*Newman et al*., 2010; *Sanford*, 2011]. Traditional calibration targets include

hydraulic head data, discharge rates, and stream flow data. Unconventional calibration targets obtained from environmental tracers that have been applied in previous studies include age and travel times [*Reilly et al*., 1994; *Goode*, 1996], solute distributions [*Christensen et al*., 1995; *Anderman et al*., 1996], temperature [*Anderson*, 2005], or a combination of these targets [*Sanford et al*., 2004; *Manning and Solomon*, 2005]. These studies have clearly demonstrated the value of tracer-based calibration targets for reducing the uncertainty of model results and minimizing model nonuniqueness. In mountainous terrain, noble gas concentrations can be used to estimate the elevation where groundwater recharged (recharge elevation). The water table temperature at the recharge location (recharge temperature) can be computed from measured gas concentrations, and this recharge temperature can then be converted to a recharge elevation based on a known relationship between ground temperature and elevation [*Aeschbach-Hertig et al*., 1999; *Manning and Solomon*, 2003]. Though clearly valuable for developing conceptual models in mountain areas, noble-gas-derived recharge elevations have never been used to calibrate a numerical groundwater model to our best knowledge.

The objective of this study is to determine if recharge elevations derived from noble gas concentrations can help constrain and calibrate a regional groundwater flow model. We develop a conceptual and a numerical model for an alluvial aquifer in a humid, mountainous region in Gibsons, British Columbia, located on the south-westernmost region of the Coast Mountains in Canada. Since most studies of mountain block recharge have focused on arid or semiarid regions within continental interiors, an additional contribution of this study is quantifying mountain block recharge in a humid, coastal environment.

2. Study Area

The field area is the Town of Gibsons, a coastal community in southwestern British Columbia, Canada (Figure 1a) surrounded by Howe Sound, the Georgia Strait and Mt. Elphinstone, part of the Coast Mountains. The average annual precipitation rate to the Town is 1369 mm/yr [*Environment Canada*, 2012]. Groundwater from the Gibsons aquifer supplies 73% of its 4473 residents [*Statistics Canada*, 2011], and is an invaluable resource to this rapidly growing town. However, recharge to the Gibsons aquifer and the long-term sustainability of the town's water supply are not well understood. The town supply wells are all located in Lower Gibsons (Figure 1b), where the aquifer is confined and has flowing artesian conditions. Three (TW1, TW3, and TW4) of the four supply wells are active and one (TW2) is used for back-up. A monitoring well network (Table 1) includes the four supply wells, two private supply wells (70651 and Strata), two nested piezometers (MW06-1 and MW06-2) and three deep monitoring wells (WL10-01, WL10-02, and School Board).

Local bedrock geology consists of early Middle Jurassic Bowen Island Group metasediments and metavolcanics with Late Jurassic and Early Cretaceous intrusions of quartz-diorite and granodiorite that underlie most of the town (Figure 2) [*Friedman et al*., 1990; *Monger*, 1994; *Monger and Journeay*, 1994]. A sharp contact between the Bowen Island Group and the Late Jurassic granodiorite runs along the lower reaches of Gibsons Creek and trends northwest along the base of Mt. Elphinstone. Quaternary sediments up to 300 m thick underlay the lowlands bordering the Strait of Georgia, referred to as the Georgia Lowlands. Within the study area, the following deposits have either been mapped at the surface or recorded in drill logs in stratigraphic order starting with the oldest (Figure 2): (1) The Gibsons aquifer (also called herein by its more formal geological name, Pre-Vashon deposits) was deposited during glacial advance along the Georgia Strait [*Clague*, 1977]. Beneath the Town of Gibsons, Pre-Vashon deposits are flat-lying interbeds of silt, sand and gravel that sit nonconformably on top of bedrock. (2) Vashon Drift sediments (generally $<$50 m thick) are glacial deposits from the Fraser Glaciation, including till, glaciofluvial and glaciolacustrine sediments composed of hard packed silt, clay, sand, gravel, and stones that confine the Gibsons aquifer. (3) Capilano sediments are retreat-phase glaciofluvial, glaciomarine, and marine sediments deposited on the seafloor and as raised deltas, intertidal and beach sediments [*Armstrong*, 1981]. (4) Salish sediments are postglacial to recent deposits at current sea level deposited through fluvial, lacustrine, deltaic, shoreline, or eolian geomorphic processes [*Fyles*, 1963]. In Gibsons, Salish sediments are mapped along creek beds and the shoreline.

Figure 2 illustrates the hydrostratigraphy and conceptual model of the Gibsons aquifer; the extent and thickness of the Pre-Vashon sediments and piezometric surface of the Gibsons aquifer are shown in Figure 1b. The Vashon till and the basal marine/glaciomarine Capilano deposits are combined herein as the

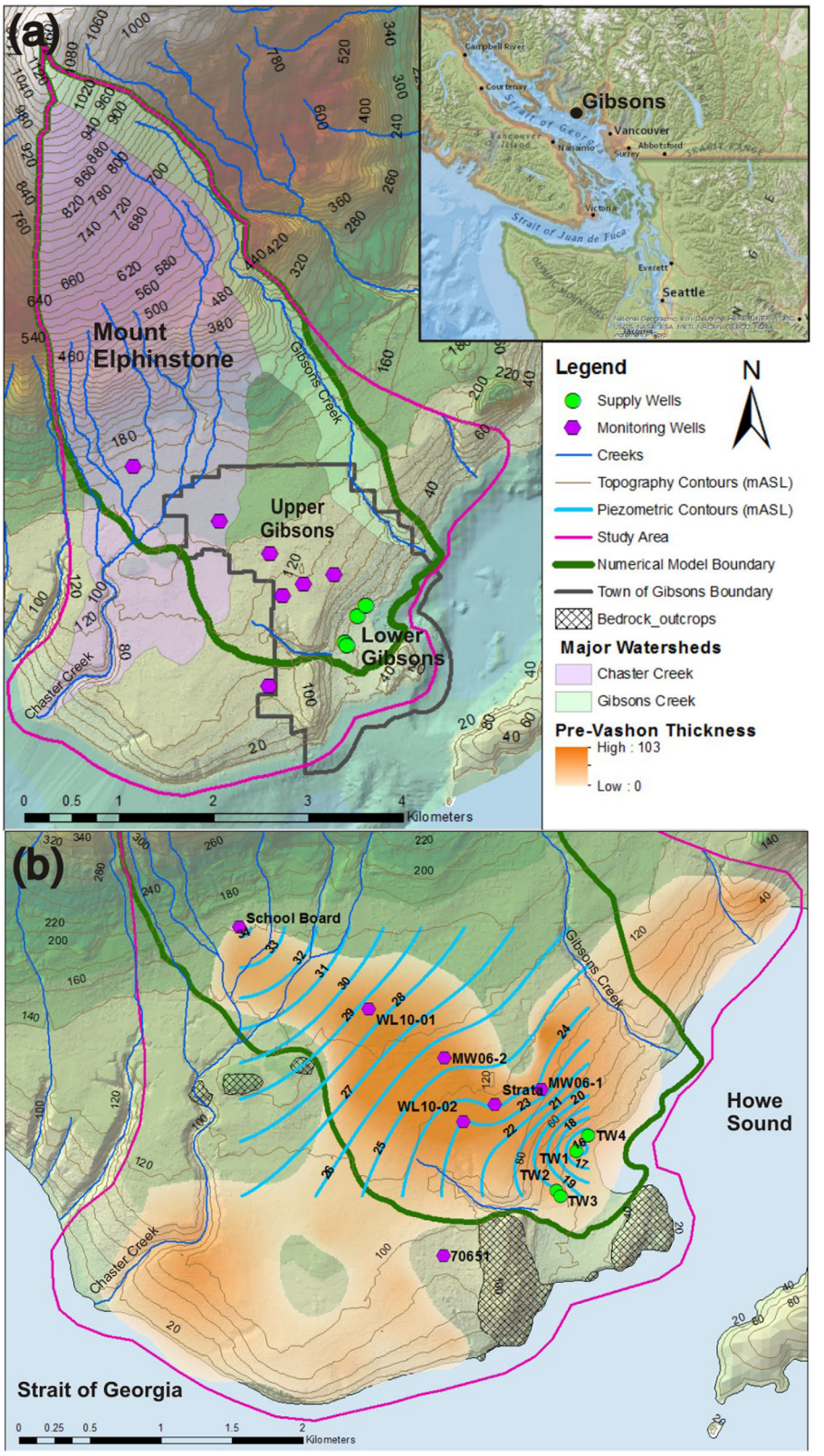

Figure 1. (a) The study area is defined by the two major watersheds that encompass the Gibsons aquifer. (b) The extent and thickness of the pre-Vashon deposits containing the Gibsons aquifer and the piezometric surface. The numerical model boundary is defined by the watershed boundaries (topographic devides) or by bedrock highs and or outcrop.

Table 1. Summary of Wells Included in the Groundwater Monitoring Network[a]

Well Name	Description	Easting	Northing	Ground Elevation (mASL)	Well Depth (mBGL)	Screen Top (mBGL)	Screen Bottom (mBGL)	Hydro-Stratigraphic Unit	Water Level (mBTOC)	Range of Measured K Values (m/s)
School Board	MW	460,524	5,473,736	153	139	Unknown	Unknown	Pre-Vashon	101.5	
MW06-1A	NP	462,812	5,472,468	99.5	78	74.4	77.7	Pre-Vashon	74.9	
MW06-1B	NP	462,812	5,472,468	99.5	78	3.3	12.3	Capilano	3.9	
MW06-2A	NP	462,130	5,472,688	121.5	102	98.9	101.9	Pre-Vashon	97.2	
MW06-2B	NP	462,130	5,472,688	121.5	102	11.3	14.3	Capilano	2.9	
WL10-01	MW	461,597	5,473,033	139.5	141	137.2	140.2	Pre-Vashon	140.2	4.9×10^{-4} to 9.6×10^{-5}
WL10-02	MW	462,263	5,472,238	107.5	123	120.4	123.4	Pre-Vashon	123.4	3.5×10^{-3} to 1.3×10^{-4}
TW 1	WSW	463,057	5,472,034	12.7	42	19.8	22.9	Pre-Vashon	Artesian	
TW 2	WSW	462,924	5,471,757	18	15	13.1	14.6	Pre-Vashon	Artesian	
TW 3	WSW	462,943	5,471,715	18.5	26	21	24.5	Pre-Vashon	Artesian	
TW 4	WSW	463,143	5,472,141	13	20	11.9	15.5	Pre-Vashon	Artesian	1×10^{-2} to 1×10^{-4}
70651	PW	462,156	5,471,290	93	116	10	93	Bedrock	NM	
Strata	PW	462,486	5,472,360	110.5	Unknown	Unknown	Unknown	Pre-Vashon	87.6	

[a]Abbreviations: mASL, meters above sea level; mBGL, meters below ground level; mBTOC, meters below top of casing; MW, monitoring well; NP, nested piezometer; WSW, water supply well; PW private pumping well; and NM, not measured.

"Vashon till aquitard" since both have aquitard properties. The Vashon till aquitard varies in thickness from a few meters thick in Lower Gibsons to greater than 50 m thick toward the base of Mt. Elphinstone. Beneath the Upper Gibsons "bench" the Gibsons aquifer becomes partially saturated and the depth to the top of the water table can exceed 100 m below ground. The unconfined Capilano aquifer (<10 m thick) is perched on top of the Vashon till within the Capilano intertidal beach sediments along most of Upper Gibsons.

Groundwater recharge, flow, and discharge for the Gibsons aquifer are not well constrained. Recharge to the Gibsons aquifer may occur through creeks, gaps, or as vertical leakage through the Vashon till. Two zones of potential recharge that have not been carefully investigated before this study are the Capilano

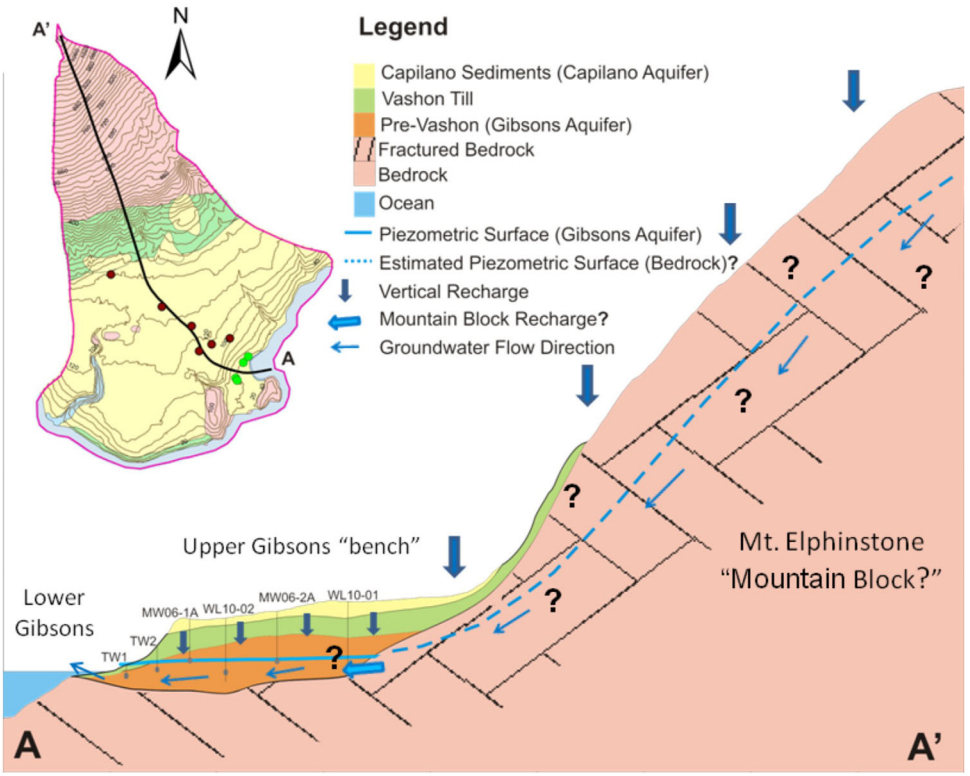

Figure 2. Conceptual cross section A–A′ through the Gibsons aquifer demonstrating where the aquifer is flowing artesian, partially unconfined, and the uncertainty of the role of mountain block recharge.

deposits near the base of Mt. Elphinstone, and Mt. Elphinstone itself (the source of mountain block recharge). Fractures in intrusive rocks have been recorded in well logs within the study area some of which are water-bearing. Groundwater within the Gibsons aquifer generally flows northwest to southeast following topography (Figure 1b). Measured aquifer hydraulic conductivity (K) values are generally on the order of 10^{-4} m/s (Table 1). This relatively high K within the Gibsons aquifer is consistent with a relatively low regional hydraulic gradient (0.006) coupled with flowing artesian conditions in the Town of Gibsons supply wells. The average linear groundwater velocity based on Darcy's Law is ~350 m/yr, suggesting that groundwater in the Gibsons aquifer should be modern (<60 year old). Most of the groundwater within the Gibsons aquifer that is not extracted by wells is assumed to discharge directly to the ocean, through several springs observed along the coastline, or into incised creeks near the shoreline.

3. Methods

3.1. Sampling and Laboratory Analysis

Groundwater or gas samples were collected from wells in April 2011 for tritium (^{3}H), and noble gases (He, Ne, Ar, Kr, Xe). Details beyond the summary below can be found in *Doyle* [2013]. All wells were purged until field parameters (temperature, pH, and electrical conductance) stabilized prior to sampling. Wells with dedicated pumps were purged by pumping and wells without dedicated pumps were purged by bailing. Samples for noble gases were collected as either water samples in copper tubes using standard methods [*Stute and Schlosser*, 1993] or as gas samples using advanced diffusion samplers left in the well for a week [*Gardner and Solomon*, 2009]. Noble gases were analyzed at the University of Utah Dissolved and Noble Gas Laboratory in 2012. The abundance of Ne, Ar, Kr, and Xe were measured using a Stanford Research SRS Model RGA 300 quadrupole mass spectrometer. Helium-3 (^{3}He) and helium-4 (^{4}He) were measured using a Mass Analyzers Products Model 215-50 Magnetic Sector Mass Spectrometer. ^{3}He and ^{4}He results are reported as total ^{4}He and R/R_a, where R is the measured $^3He/^4He$ ratio in the sample and R_a is the atmosphere $^3He/^4He$ ratio [*Clarke et al*., 1976]. Measurement uncertainty (1σ) is 1% for ^{4}He and R/R_a, 2% for Ne and Ar, and 5% for Kr and Xe. Tritium was measured using the helium ingrowth method [*Bayer et al*., 1989], with ingrown ^{3}He being measured on the same magnetic sector MS as above.

3.2. ^{3}H/^{3}He Age and Recharge Elevation

Recharge temperature (T_r) and excess air parameters A_e and F were computed from measured noble gas concentrations (Ne, Ar, Kr, and Xe) assuming the closed-system equilibrium (CE) model of excess air formation, where A_e is the initial amount of trapped air and F is the degree of fractionation during dissolution of that air [*Aeschbach-Hertig et al*., 2000]. Recharge parameters were derived for each sample by minimizing the error-weighted misfit between all measured and modeled gas concentrations (χ^2) simultaneously, using a computer code described in *Manning and Solomon* [2003] based on methods detailed in *Aeschbach-Hertig et al*. [1999] and *Ballentine and Hall* [1999]. A recharge elevation (H) must be assumed in order to compute T_r. Initially, recharge parameters were computed for each sample assuming H equal to the well head elevation for the purpose of evaluating the consistency of the resulting T_r with low-elevation water table temperatures, and computing the different ^{4}He and ^{3}He components required for calculating a ^{3}H/^{3}He age. These He components include the terrigenic component of ^{4}He ($^4He_{terr}$), which accumulates in groundwater due to radioactive decay of uranium and thorium in crustal rocks [*Solomon and Cook*, 2000]. In general, longer groundwater residence times result in higher $^4He_{terr}$ concentrations. ^{3}H/^{3}He ages were calculated using standard methods described by *Schlosser et al*. [1988, 1989] and *Solomon and Cook* [2000].

Recharge temperatures were used to constrain H using the approach described in *Aeschbach-Hertig et al*. [1999], *Manning and Solomon* [2003], *Manning* [2011], and *Heilweil et al*. [2012]. Throughout this paper, all samples are assumed to be mixtures of waters recharged at different elevations. This means that the T_r and H values mentioned below are mean values rather than single values associated with a homogeneous sample containing only water recharged at a single elevation. Similarly, minimum and maximum values for T_r and H refer to the range of possible mean T_r and mean H values.

For each sample, the range of possible T_r values was computed. A minimum T_r (T_{rmin}) was computed assuming the maximum possible H (H_{max}, the top of Mt. Elphinstone at 1160 mASL), and a maximum T_r (T_{rmax}) was computed assuming the minimum possible H (H_{min}, the well head elevation). On a plot of T_r versus H, shown in Figure 3, a line connecting the points (T_{rmax}, H_{min}) and (T_{rmin}, H_{max}) is termed as a "sample line"

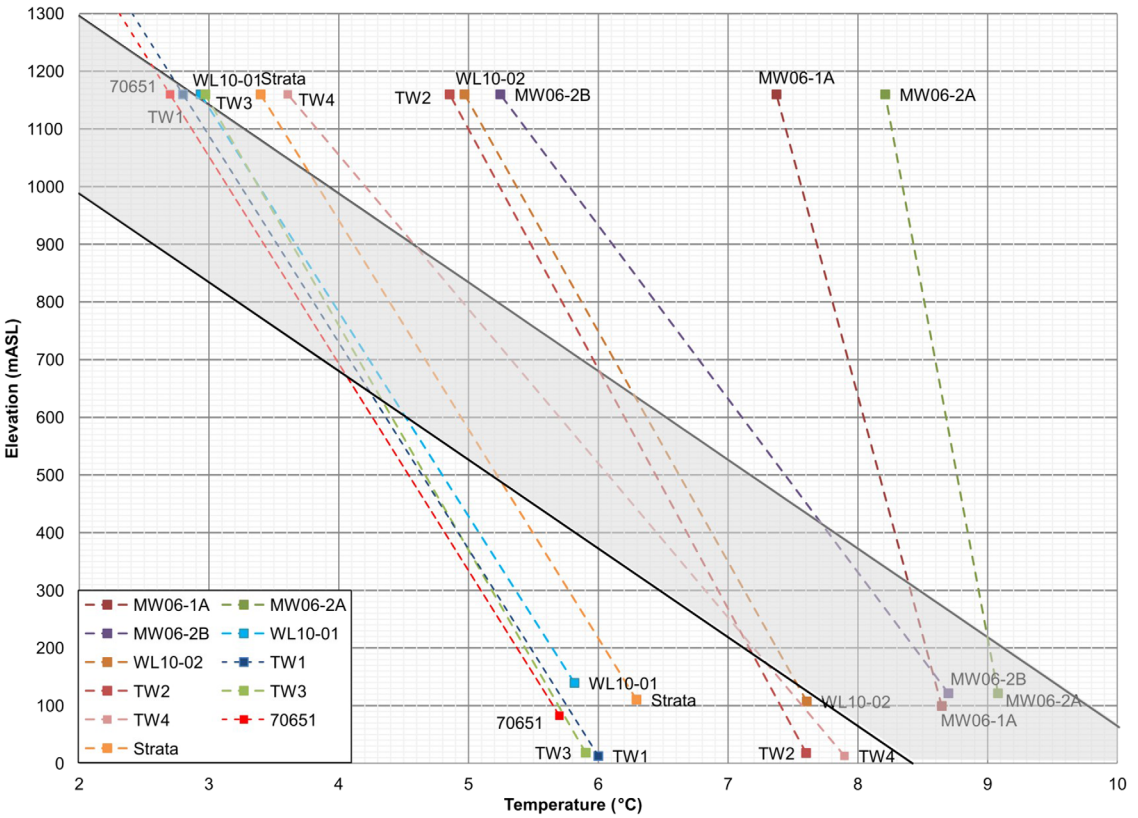

Figure 3. Possible combinations of noble gas recharge temperature and recharge elevation (sample lines) for each sample. Maximum (T_{rmax}) and minimum (T_{rmin}) recharge temperatures were computed assuming the minimum (H_{min}) and maximum (H_{max}) recharge elevations for each sample, respectively. H_{min} is the elevation at the well head from which the sample was collected, and H_{max} for all samples is the elevation at the top of Mt. Elphinstone (1160 mASL). Gray zone defines the local T_r lapse, defined by the atmospheric lapse minus 0–2°C. Intersection of a sample line and the gray zone provides a best estimate for the mean H range for each sample.

and defines the range of possible $T_r - H$ pairs for the sample. The T_r lapse (relationship between H and T_r) for the study area was assumed to equal the local atmospheric lapse (relationship between elevation and mean annual air temperature, T_{atm}) minus 0–2°C. A linear atmospheric lapse of $T_{atm} = -0.0065z + 10.4$ was assumed (where z is elevation in mASL and T_{atm} is in °C), based on a T_{atm} of 10.2°C recorded at the Gower Point meteorological station at 34 mASL [*Environment Canada*, 2012], and a typical lapse rate of 6.5°C/1000 m of elevation gain. Recharge temperature was assumed to be 0–2°C below T_{atm} based on the findings by *Manning and Solomon* [2003], *Manning* [2011], and *Masbruch et al.* [2012] who showed that T_r in crystalline-rock mountain blocks with significant winter snowpacks is typically in this range. When the local T_r lapse is plotted on the same plot as the sample lines, the intersection of a sample line and the T_r lapse defines the range of likely H values for that sample.

One concern regarding this approach is uncertainty in the validity of a T_r value computed for a mixed sample composed of waters of varying T_r and excess air composition. The question of how closely the computed T_r approximates the actual mean T_r for a mixed sample has not been directly addressed in previous studies. Concern stems from the fact that apparent groundwater ages computed from dissolved gas tracers and ^{3}H for a mixed-age sample can be very different from the sample's actual mean age.

To address this concern, the following Monte Carlo experiment was performed. Three thousand synthetic mixed samples were generated, each containing two theoretical waters combined in randomly varying proportions. Each of these two waters had a randomly assigned H of 100–1160 mASL, A_e of 0.1–0.001 cm^3 STP/g, and F of 0.0–1.0, these ranges being consistent with site conditions. The T_r of each water was assigned using H and the mean T_r lapse for the site ($T_{atm} - 1$°C). Total excess air concentration was constrained to $<$0.01 cm^3 STP/g, also consistent with site conditions. Concentrations of Ne, Ar, Kr, and Xe were computed for each water using the CE model. Recharge temperature was then computed for each synthetic sample (assuming the CE model) and compared to the actual mean sample T_r. Results of the experiment are shown in Figure 4.

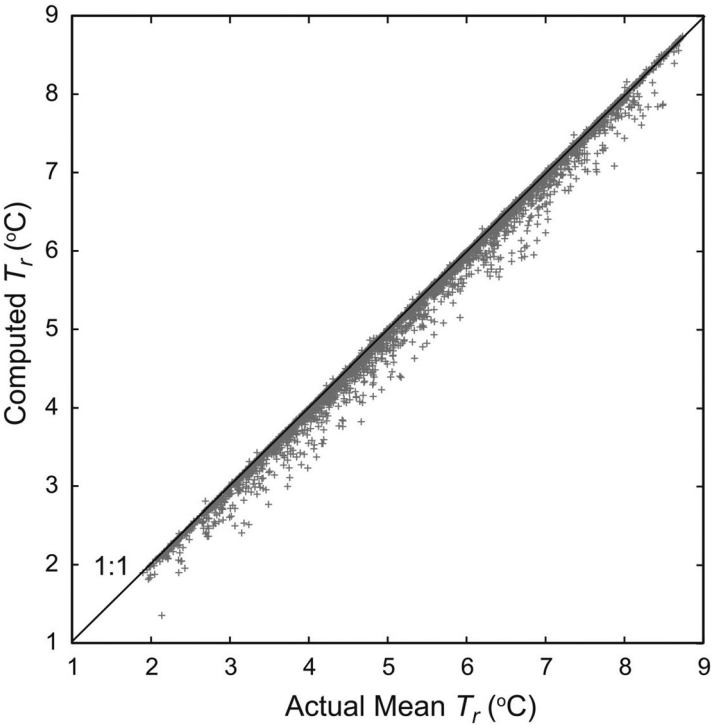

Figure 4. Computed noble gas recharge temperature versus actual mean recharge temperature for 3000 synthetic mixed samples generated using a Monte Carlo approach. 97% of samples agree within 0.5°C.

Computed and actual mean T_r values agree within 0.5°C for 97% of the samples. Computed T_r values have a consistent cold bias, but this is generally smaller than the uncertainty in T_r related to gas measurement errors (1–2°C). Discrepancies between computed and actual mean T_r are thus acceptably small for the purposes of this study.

3.3. Numerical Modeling

A numerical groundwater flow model was constructed using the commercial software package Visual MODFLOW 2009.1 [*Reilly and Harbaugh*, 2004], which uses the finite difference code MODFLOW-2000, developed by the United States Geological Survey to solve the saturated groundwater flow equation. Given the regional nature of the study area and the available input and calibration data available, MODFLOW is a suitable numerical model code to use. Because of the lack of physical data in the mountain block, such as drilled boreholes, well logs or fracture data, at the regional scale it is more appropriate to model flow through fractured bedrock as an equivalent porous medium rather than as discrete-fracture networks [e.g., *Kahn et al*., 2008]. A solute transport model was not used to simulate noble gas concentrations explicitly because it was determined that calibrating the model to noble-gas-derived recharge elevations (rather than directly to gas concentrations) was a better approach for reasons explained below.

The model domain extends from the top of Mount Elphinstone to the ocean (Figure 1a). The model domain is defined by the watershed catchment boundaries in the northwest and by the thickest deposits of the Pre-Vashon sediments containing the Gibsons aquifer in the southeast. The top of the model is at the land surface, not the water table. The grid consists of 140 rows, 70 columns, and 5 layers with uniform 50 m × 50 m grid cells in the x and y directions. Grid layers were specified according to geology but edited to be continuous, have a minimum thickness of 10 m, and have enough overlap with horizontally adjacent cells to minimize numerical instability. The model domain was oriented 45° to the east to align the grid with the principal direction of groundwater flow (northeast to southwest).

The steep topography and unconfined nature of the upper portion of the aquifer made it necessary to run the model with cell wetting activated. Dry cells were reactivated if the head below the dry cell is 0.1 m above the bottom of the dry cell and head values were calculated from heads in the surrounding active cells. Rewetting calculations were conducted every iteration required to solve the steady state model. Additional modeling details are described in *Doyle* [2013].

Boundary conditions applied to the model are shown in Figure 5. No flow boundaries were assigned to the base of the model, the lateral boundaries, and to the surface of the model over the area where the Gibsons aquifer has fully confined conditions. A constant head of 0 mASL was applied to layer one along the ocean to represent the average long-term sea level. Recharge was applied as a constant downward vertical flux to the uppermost active layer of the model. Three recharge zones were created based on orographic precipitation patterns, surface geology, slope, elevation, and proximity to snow accumulation and or snow melt (Figure 5). Groundwater from the aquifer is extracted by three active Town supply wells and one private well.

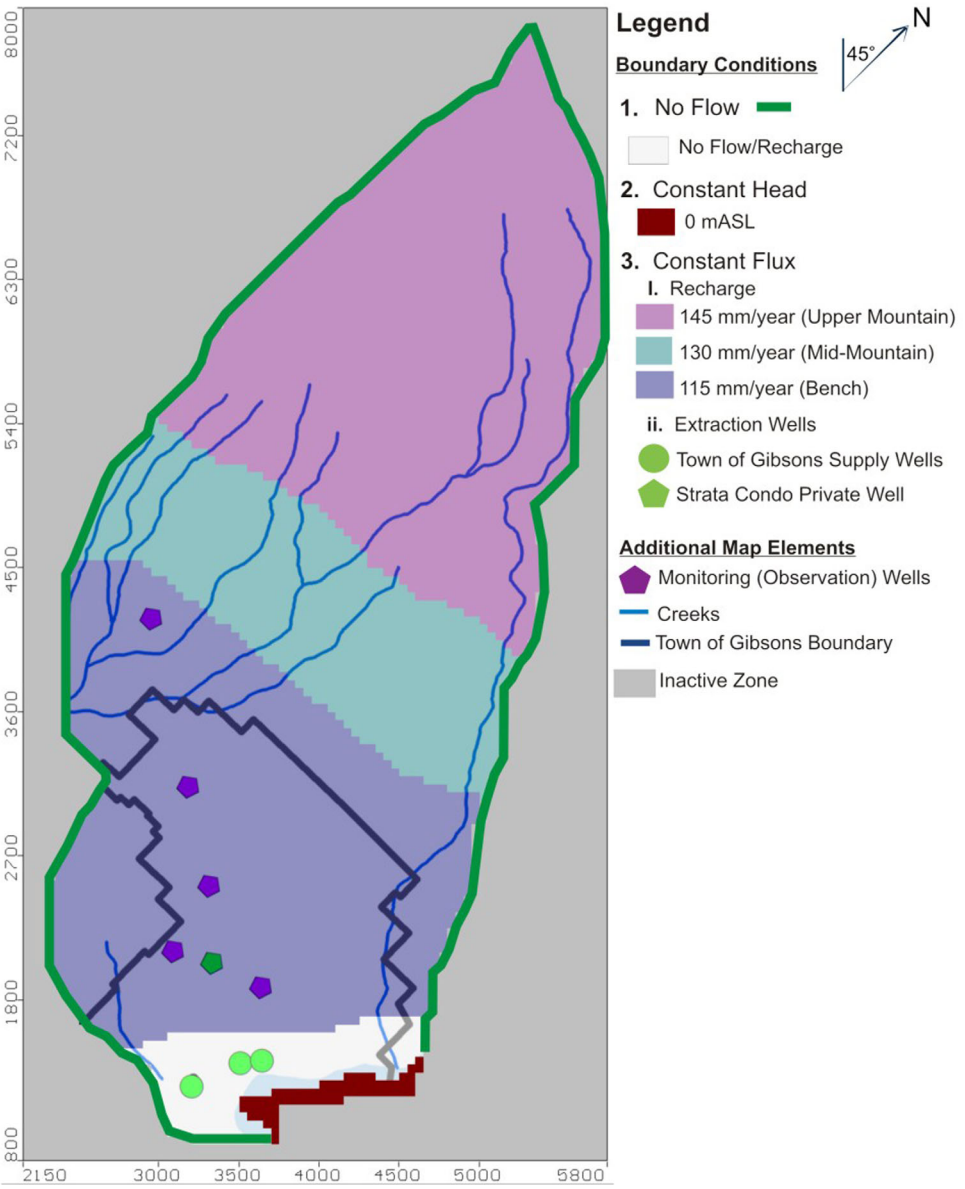

Figure 5. Boundary conditions and zones of recharge. Recharge rates shown are final calibrated values for the best fit model.

Steady state pumping rates of 338.0, 1667.1, and 271.1 m^3/d were calculated by averaging 3 years (2009–2011) of groundwater extraction data recorded from TW1, TW3, and TW4, respectively [*Doyle*, 2013]. An average groundwater extraction rate of 100 m^3/d was assumed for the Strata well, used only to supply water to a fountain.

The spatial distribution of the hydraulic conductivity zones (Figure 6) was specified according to geological layers and values of hydraulic conductivity by historic pump tests, slug tests, grain size analyses, or values recorded in the literature (Table 1) [*Doyle*, 2013]. Values and distribution of the hydraulic conductivity zones were refined during the calibration process. Previous modeling studies of mountain block groundwater flow have represented K within the mountain block as either a constant value [e.g., *Smerdon et al*., 2009] or as decreasing with depth [e.g., *Manning and Solomon*, 2005]. Multiple studies summarized by *Manning and Solomon* [2005] and more recently by *Welch and Allen* [2014] support a conceptual model in which a near-surface high-conductivity "active layer" overlies a deeper, low-conductivity "inactive layer," where the former is likely to have a higher density of fractures that could be caused by weathering, unloading, exfoliation, or the enhancement of fractures by surficial movement. In these studies, measured and modeled K

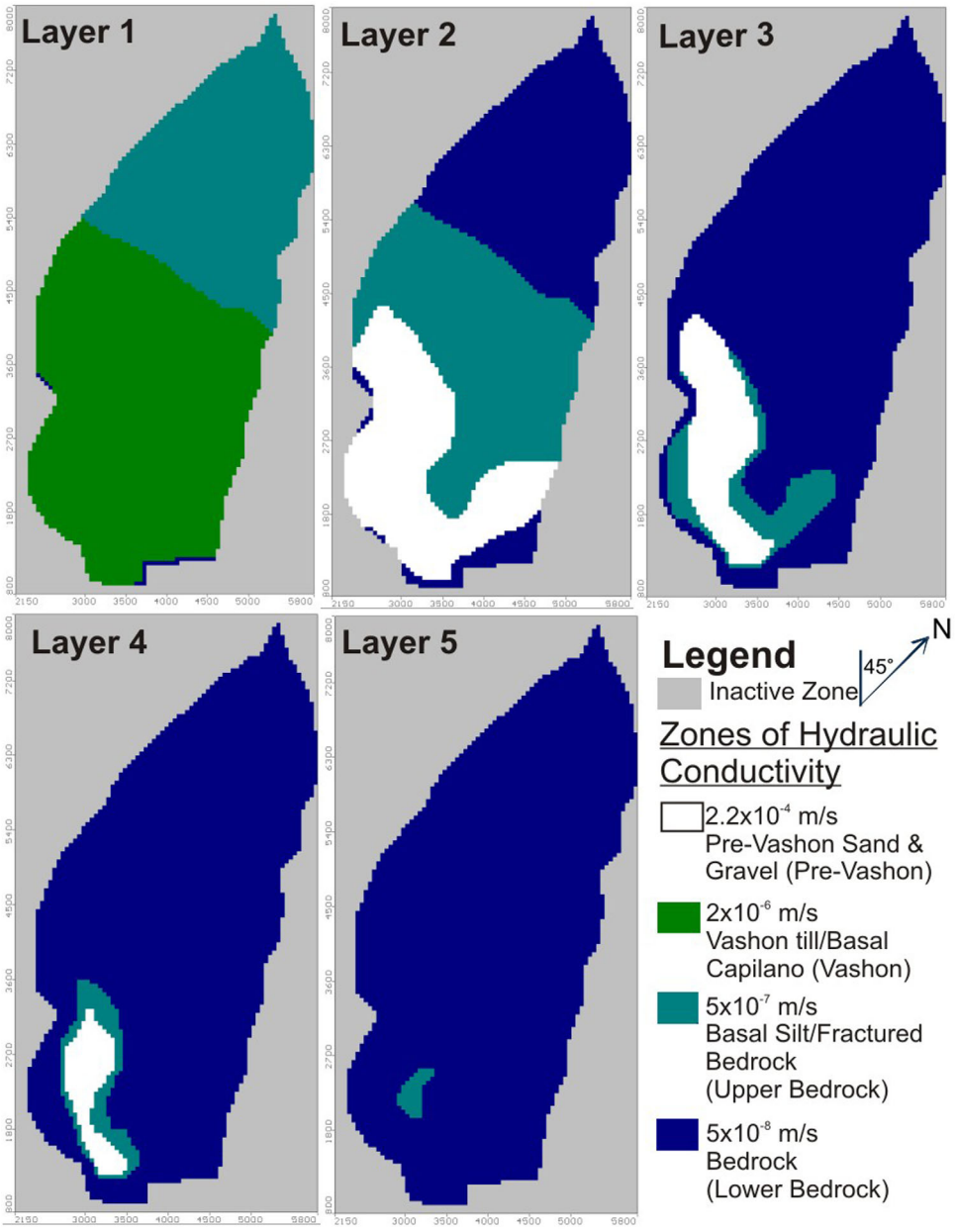

Figure 6. Final calibrated zones of hydraulic conductivity specified in each of the five layers of the best fit model.

values in the active layer are typically on the order of 10^{-8} to 10^{-6} m/s. In this study, a basal silt/upper fractured bedrock layer, referred to as "upper bedrock," is used to represent an active layer. The thickness of the active layer varies due to the steepness of the elevation, however, ranges between approximately 200 m thick at the top of the mountain and 10 m thick near the ocean.

The model was calibrated to conventional average long-term hydraulic head data (Table 1) in all monitoring wells. Because there are no dedicated nonpumping monitoring wells located in Lower Gibsons, the average pumping water level recorded in TW4 was also included as a calibration target. TW4 was the most suitable pumping well to use as it is the most recently drilled Town supply well and thus least affected by wellbore inefficiency (long-term permeability reduction near the wellbore).

The MODPATH/MODPATH-PLOT package in MODFLOW was used to calibrate to recharge elevation by computing and displaying three-dimensional particle path lines. Ten backward-tracking particles were released

from evenly distributed points along the full length of well screens for all wells that were sampled and analyzed for noble gases. It was assumed that the termination points of the backward-tracking particles mark the recharge location of groundwater that flows to each well. The elevation of the surface of the model directly above the termination point of each of the 10 particles was used to compute the mean recharge elevation for the well. The modeled mean recharge elevation was then compared to the range of mean H values computed from the noble gas concentrations.

An alternate and more direct calibration approach was considered involving using the particle tracks to model noble gas concentrations in sampled wells explicitly (assuming purely advective transport), and directly comparing these to measured gas concentration. However, preliminary calculations indicated that this approach would provide less constraint on recharge elevation because the dependence of the gas concentrations on H is generally weaker than the dependence of T_r on H. Whereas the solubility component of the gas concentration is directly dependent on H, the excess air component is not, and excess air can compose a large fraction of the total gas concentration. As a result, ranges of possible gas concentrations at the highest and lowest elevations at the site are quite similar, overlapping 47% (Xe) to 100% (Ne). Our approach of employing T_r takes advantage of our ability to identify and subtract out the excess air component and utilize the elevation-dependent solubility component alone.

The model was calibrated using a manual, iterative process whereby values and distribution of K and recharge were adjusted until calibration to both observed water levels and recharge elevations were achieved. Values of hydraulic conductivity representing each hydrolithological unit were varied within the measured, historical, or compiled literature value ranges. The spatial distribution of each conductivity zone was only modified in areas where well logs, geophysics, or mapped geology were not available to constrain the subsurface geology. Hydraulic conductivity representing bedrock was the least constrained. Recharge rates were varied within the range of typical recharge rates determined from previous studies of similar climates and recharge conditions.

Measured ^{3}H and ^{3}He were not employed in model calibration for three reasons. First, groundwater age is dependent upon the porosity of material along the groundwater flow path, and the effective porosity of the fractured rock composing the mountain block is unknown and could vary over orders of magnitude [*Manning and Solomon*, 2005]. It is, therefore, likely that many of the measured ages (or measured ^{3}H and ^{3}He concentrations) could be matched in the model by either adjusting recharge rates or mountain block porosity. Second, diffusive exchange of He between actively flowing fracture water and immobile (older) matrix water in the mountain block could lead to a loss of tritiogenic ^{3}He [*Cook et al*., 2005]. The effect of this matrix diffusion on the ^{3}He concentration (and ^{3}H/^{3}He age, ^{4}He concentration, and possibly ^{3}H as well) could only be accounted for by employing a discrete-fracture solute transport model, and insufficient data are available to do so at this site. Note that matrix diffusion is probably not a concern for the other noble gas concentrations because these have remained nearly constant in the atmosphere for thousands of years, so fracture and matrix waters should be in equilibrium. Third, several of the samples probably contain a fraction of premodern ($>$60 year old) water, meaning that the ^{3}H/^{3}He age likely underestimates the true sample mean age by an unknown amount. Although these concerns render ^{3}H, ^{3}He, and ^{3}H/^{3}He age unreliable for model calibration, apparent ^{3}H/^{3}He ages are still useful for identifying general/relative groundwater age relationships and conceptual model development.

Zone budgets were assigned in MODFLOW to calculate the contribution of mountain block recharge and the overall recharge to the Gibsons aquifer. Zones were assigned according to the three zones of recharge (Figure 5). Mountain block recharge was identified as the flux of water flowing across a vertical cut between the upper-mountain and midmountain zones, where the aquifer begins to abut onto the mountain.

A sensitivity analysis was performed to assess how uncertainties in the input values affect the model outputs. Two approaches to the sensitivity analysis were taken: (1) values of hydraulic conductivity and recharge were adjusted by $\pm$50%, in order to assess the impact on modeled heads (water table elevation), recharge elevation and the percent of mountain block recharge (% mountain block recharge), and (2) the geometry of the bedrock surface was adjusted in order to assess its effect on hydraulic heads and recharge elevation since the bedrock geometry is poorly constrained. Although these adjustments do not cover all plausible uncertainties in the model, they do cover uncertainty of all input parameters and are based on model conceptualization.

Table 2. Measured Tracer Data[a]

Well Name	Sampling Method	Sample Depth (mBGL)	Length of Equilibrium Time in Well	Ar Total (cm^3 STP/g)	Ne Total (cm^3 STP/g)	Kr Total (cm^3 STP/g)	Xe Total (cm^3 STP/g)	^{4}He Total (cm^3 STP/g)	R/Ra	^{3}H (TU)
MW06-1A	ADS	77	11 days	4.38E-04	2.29E-07	9.43E-08	1.45E-08	5.26E-08	1.07	2.65
MW06-2A	ADS	101	7 days	4.45E-04	2.27E-07	9.15E-08	1.45E-08	5.33E-08	1.09	4.86
MW06-2B	ADS	14	7 days	4.19E-04	2.46E-07	1.02E-07	1.37E-08	5.69E-08	1.00	3.31
WL10-01	ADS	139	10 days	4.88E-04	2.89E-07	1.11E-07	1.57E-08	1.00E-07	0.83	0.05
WL10-02	ADS	122	9 days	4.67E-04	2.51E-07	1.03E-07	1.53E-08	6.79E-08	1.36	3.52
TW#1	PCCT			4.54E-04	2.39E-07	1.08E-07	1.55E-08	5.57E-08	1.59	3.93
TW#2	PCCT			4.41E-04	2.43E-07	9.88E-08	1.44E-08	5.23E-08	1.41	5.67
TW#3	PCCT			4.63E-04	2.46E-07	1.09E-07	1.56E-08	5.43E-08	1.34	4.28
TW#4	PCCT			4.13E-04	2.30E-07	1.02E-07	1.44E-08	5.37E-08	1.31	5.54
70651	PCCT			4.97E-04	3.15E-07	1.16E-07	1.57E-08	7.79E-08	0.99	1.77
Strata	PCCT			4.45E-04	2.52E-07	1.08E-07	1.50E-08	5.42E-08	1.24	6.62

[a]Abbreviations: mBGL, meters below ground level; ADS, advanced diffusion sampler; and PCCT, pumped clamped copper tube.

4. Results and Discussion

4.1. Recharge Parameters and ^{3}H/^{3}He Ages

Analytical results for tritium, noble gas, and He isotope analyses are summarized in Table 2. Computed recharge parameters, $^4He_{terr}$ concentrations, and $^3H/^3He$ ages are shown in Table 3. Recharge parameter model fits are generally good, with χ^2 values for most samples indicating a probability >0.05.

Calculated T_r values range from 5.7°C to 9.1°C when H is assumed equal to the well head elevation. Uncertainties for T_r generally range from 1°C to 2°C [*Doyle*, 2013]. The coolest T_r values were from wells 70651, WL10-01, TW3, TW1, and Strata (5.7–6.3°C). The warmest T_r values were from wells MW06-1A, MW06-2A, and MW06-2B (8.6–9.1°C). Groundwater temperatures measured during sampling (T_{mes}) were 8.4–9.3°C in wells screened in the Gibsons aquifer, 10.5°C in MW06-2B screened in the Capliano aquifer, and 9.8°C in well 70651 screened in bedrock (Table 3). As noted above, T_{atm} at the Gower Point Climate station at an elevation of 34 mASL (slightly lower than the bench elevation 100 mASL) is 10.2°C [*Environment Canada*, 2012]. In the discussion below, "low-elevation recharge" is that which occurs directly through the Capilano sediments and/or Vashon till at elevations <400 mASL, in contrast to mountain block recharge which occurs directly through fractured rock at elevations >400 mASL. Well MW06-2B is screened in a perched aquifer on top of the Vashon till, and wells MW06-1A and 2A are screened near the water table in the Gibsons aquifer. These wells, therefore, likely contain largely or entirely low-elevation recharge. Recharge temperatures for these wells are all ~9°C, suggesting that low-elevation recharge has a T_r of ~9°C. This is close to the low-elevation T_{atm} of 10.2°C (and the T_{mes} in MW06-2B of 10.5°C), as expected. The T_r of low-elevation recharge may be ~1°C cooler than T_{atm} because this recharge is dominated by rapid infiltration of rain and snowmelt during the cooler months of the year. Computed T_r values for wells 70651, WL10-01, TW3, TW1, and Strata are all ~6°C, which is ~3°C cooler than that of low-elevation recharge. These wells, therefore, apparently contain a substantial fraction of mountain block recharge that infiltrated at higher elevations. Computed T_r values for wells WL10-02, TW2, and TW4 are midrange at 7–8°C, consistent with a mixture of low-elevation

Table 3. Modeled Recharge Parameters and $^3H/^3He$ Ages

Well Name	T_{mes} (°C)	H (mASL)[a]	T_r (°C)	EA (cm^3 STP/g)	A_e (cm^3 STP/g)	F	χ^2	$^4He_{terr}$ (cm^3 STP/g)	$^3He_{trit}$ (TU)	Apparent Age (Years)
MW06-1A	8.8	99.5	8.6	0.0027	0.0847	0.86	2.03	−3.69E-11	2.5	11.8
MW06-2A	8.4	121.5	9.1	0.0031	0.1143	0.85	6.71	1.40E-10	2.9	8.3
MW06-2B	10.5	121.5	8.7	0.0027	0.0090	0.62	2.23	−1.01E-10	0.4	2.0
WL10-01	9.0	139.5	5.8	0.0061	0.0212	0.56	0.05	3.31E-08	6.8	85.8
WL10-02	8.5	107.5	7.6	0.0045	0.0660	0.78	0.47	1.04E-08	19.0	33.0
TW1	9.1	12.7	6.0	0.0025	0.0272	0.82	0.06	1.25E-09	19.1	31.4
TW2	9.0	18	7.6	0.0024	0.0547	0.87	7.92	−5.50E-10	11.9	20.1
TW3	9.2	18.5	5.9	0.0029	0.0519	0.84	1.35	−2.38E-10	10.4	21.9
TW4	8.9	13	7.9	0.0013	0.0013	0.00	1.02	1.68E-11	9.7	17.9
70651	9.8	82.6	5.7	0.0072	0.0155	0.41	0.54	3.13E-09	1.5	11.0
Strata	9.3	110.5	6.3	0.0028	0.0296	0.81	7.74	−5.06E-10	7.1	13.0

[a]Note: H is the elevation of the land surface at each well location. Abbreviation: mASL, meters above sea level.

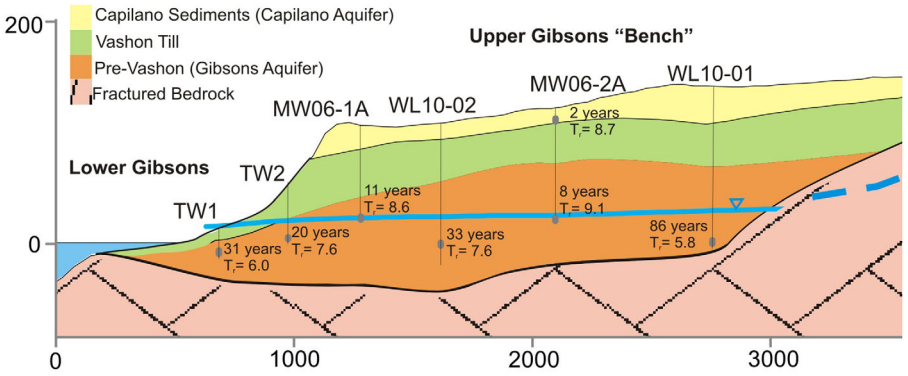

Figure 7. Schematic cross section showing apparent $^3H/^3He$ ages and noble gas recharge temperatures (T_r, in °C) calculated assuming a recharge elevation equal to well head elevation. $^3H/^3He$ ages increase and T_r values decrease with depth and with proximity to Mt. Elphinstone.

recharge and mountain block recharge. For all wells completed in the Gibsons aquifer, T_{mes} is cooler than T_{atm} by 1–2°C. This is consistent with a significant component of mountain block recharge within the aquifer. Aside from well MW06-2B, well 70651 has the warmest T_{mes} (9.8°C). This well is the only one screened in bedrock, and the warm T_{mes} may indicate deeper groundwater circulation and/or greater groundwater age compared to other wells.

Tritium concentrations range from 1.8 to 6.6 TU, indicating that the Gibsons aquifer contains dominantly modern water as expected. The one exception is well WL10-01 with a ^3H concentration of 0.05 TU, indicating all premodern water. Apparent $^3H/^3He$ ages range from 2 to 33 year (WL10-01 excluded). Apparent $^3H/^3He$ age and T_r for selected wells are displayed in the schematic cross section in Figure 7 to show their spatial distribution. Apparent $^3H/^3He$ ages increase and T_r values decrease with depth. The observed distribution suggests that the Gibsons aquifer has two primary recharge components: (1) low-elevation recharge that is modern (<10 year old) with a warm T_r (~9°C), typified by water in wells MW06-1A, MW06-2A, and MW06-2B; and (2) mountain block recharge that is premodern with a cold T_r (5–6°C), typified by water in well WL10-01, which is located at the base of the mountain block and screened directly above bedrock. Groundwater sampled from wells screened at middepth within the aquifer (WL10-02, Strata, TW1, TW2, TW3, TW4) have midrange age and T_r, and therefore apparently contain a mixture of the two recharge endmembers, or perhaps recharge from midelevations.

Total excess air (EA) was computed for each sample by summing computed excess air components for N_2, O_2, and Ar. Well WL10-01 has the highest EA concentration (0.006 cm^3 STP/g), with the exception of well 70651 (0.007 cm^3 STP/g). Well 70651 is the only well screened in bedrock, and has a low-end T_r (5.7°C) nearly equal to WL10-01. High EA concentrations have been observed in bedrock aquifers in mountain catchments where recharge is snow-melt dominated [*Manning and Caine*, 2007]. Well WL10-01 also has the highest $^4He_{terr}$ concentration (3.3×10^{-8} cm^3 STP/g), larger than the next-highest sample by about a factor of 3. This is consistent with a longer residence time in the granodiorite and metavolcanic mountain block and therefore greater accumulation of $^4He_{terr}$. The elevated EA and $^4He_{terr}$ concentrations in well WL10-01 suggest that mountain block recharge waters generally have these characteristics, along with a cold T_r and premodern age. By contrast, wells MW06-1A, MW06-2A, and MW06-2B have EA and $^4He_{terr}$ concentrations of about 0.003 and $<1 \times 10^{-9}$ cm^3 STP/g, respectively.

4.2. Recharge Elevations

The likely *H* range for each sample is defined by the intersection between the sample line and the T_r lapse zone as shown in Figure 3. The low-end *H* for the sample is where the sample line intersects the bottom of the T_r lapse zone (but not lower than the well elevation), and the high-end *H* is where the sample line intersects the top of the T_r lapse zone (but not higher than the top of Mt. Elphinstone). The estimated *H* range for each sample is shown in Table 4. As noted above, each sample is likely a mixture of waters recharged at different elevations, so the estimated *H* ranges represent the range for the mean *H* of the sample. Results indicate that a significant portion of recharge to the Gibsons aquifer probably occurs at relatively high

Table 4. $H_{min} - T_{rmax}$ and $H_{max} - T_{rmin}$ Pairs and Estimated Recharge Elevation Ranges

Well Name	H_{min} (mASL)[a]	T_{rmax} (°C)	H_{max} (mASL)	T_{rmin} (°C)	Recharge Elevation Range (mASL)	
MW06-1A	99.5	8.6	1160	7.4	99.5	310
MW06-2A	121.5	9.1	1160	8.2	121.5	220
MW06-s	121.5	8.7	1160	5.2	121.5	420
WL10-01	139.5	5.8	1160	2.9	600	1140
WL10-02	107.5	7.6	1160	5	140	640
TW1	12.7	6.0	1160	2.8	650	1180
TW2	18	7.6	1160	4.9	190	680
TW3	18.5	5.9	1160	3	630	1140
TW4	13	7.9	1160	3.6	170	900
70651	82.6	5.7	1160	2.7	670	1200
Strata	110.5	6.3	1160	3.4	490	1020

[a]Abbreviation: mASL, meters above sea level.

elevations on Mt. Elphinstone. Due to uncertainties in assumptions and T_r determinations, it should be realized that estimated H ranges are approximate and could be larger than shown in Table 4.

4.3. Best Fit Model

Calibration to recharge elevation significantly helped to constrain bedrock geometry, K values, and recharge rates and provided calibration targets along the mountain where no hydraulic head data exists. These parameters were adjusted until a best fit solution was achieved when all modeled heads fell within the acceptable error range of ± 2 m from observed heads, and when path lines from backward-tracking particles had the most overlap with the noble-gas-estimated H ranges for each well. The final calibration to hydraulic head data had a correlation coefficient of 0.993 and a normalized residual mean square of 3.6%. For most wells, the modeled mean recharge elevation falls within the H range estimated from the noble gas data. Three exceptions are wells TW1, TW2, and TW3, for which modeled recharge elevations are lower than the noble-gas-based H ranges. The reason for this discrepancy is not clear, but it could be caused by these production wells preferentially drawing water from deeper parts of the aquifer due to heterogeneities near the discharge end that are not represented in the model.

In the best fit model, 46% of recharge to the Gibsons aquifer is mountain block recharge, with a total recharge flux of 5011 m^3/d. Final calibrated K values for the different hydraulic conductivity zones are shown in Figure 6. The water table depth in the mountain block is generally 100–150 m. Approximately 8% of the total upper mountain precipitation becomes mountain block recharge. This assumes an average annual precipitation rate of 1369 mm/yr, measured along the bench. Because precipitation generally increases with elevation due to orographic effects, precipitation is likely higher along the midmountain and upper-mountain. Therefore, 8% of mountain precipitation is an upper limit for mountain block recharge. Although higher precipitation could lead to higher recharge rates in the midmountain and upper-mountain, in mountainous fractured bedrock terrain, bedrock permeability and slope may have a greater control over recharge rates than total precipitation [*Forster and Smith*, 1988].

The computed fraction of mountain precipitation that becomes mountain block recharge is on the lower end compared to previous published mountain block recharge studies. These fractions are highly variable. Compilations by *Magruder et al.* [2009] and *Wilson and Guan* [2004] indicate a low-end of 0.2% [*Chavez et al.*, 1994a, 1994b] in the Santa Catalina Mountains, Arizona, a high-end of 70% [*Gannett et al.*, 2001] in the Cascades Range, Oregon, and multiple studies reporting 10–40%. The majority of previous studies are conducted in arid to semiarid climates. The contrast between the high fraction computed by *Gannett et al.* [2001] and the relatively low fraction computed in this study is curious, given that the two study sites have similar Pacific Northwest climates. However, multiple factors control the fraction of mountain precipitation that becomes mountain block recharge [*Gleeson and Manning*, 2008; *Welch and Allen*, 2012, 2014] and the difference between mountain block recharge at the two sites is likely the result of differences in the geology and topography of the mountain block.

4.4. Sensitivity Analysis

To gain a more comprehensive understanding of the value of noble-gas-derived recharge elevations in model calibration, a sensitivity analysis was performed by independently adjusting each zone of hydraulic

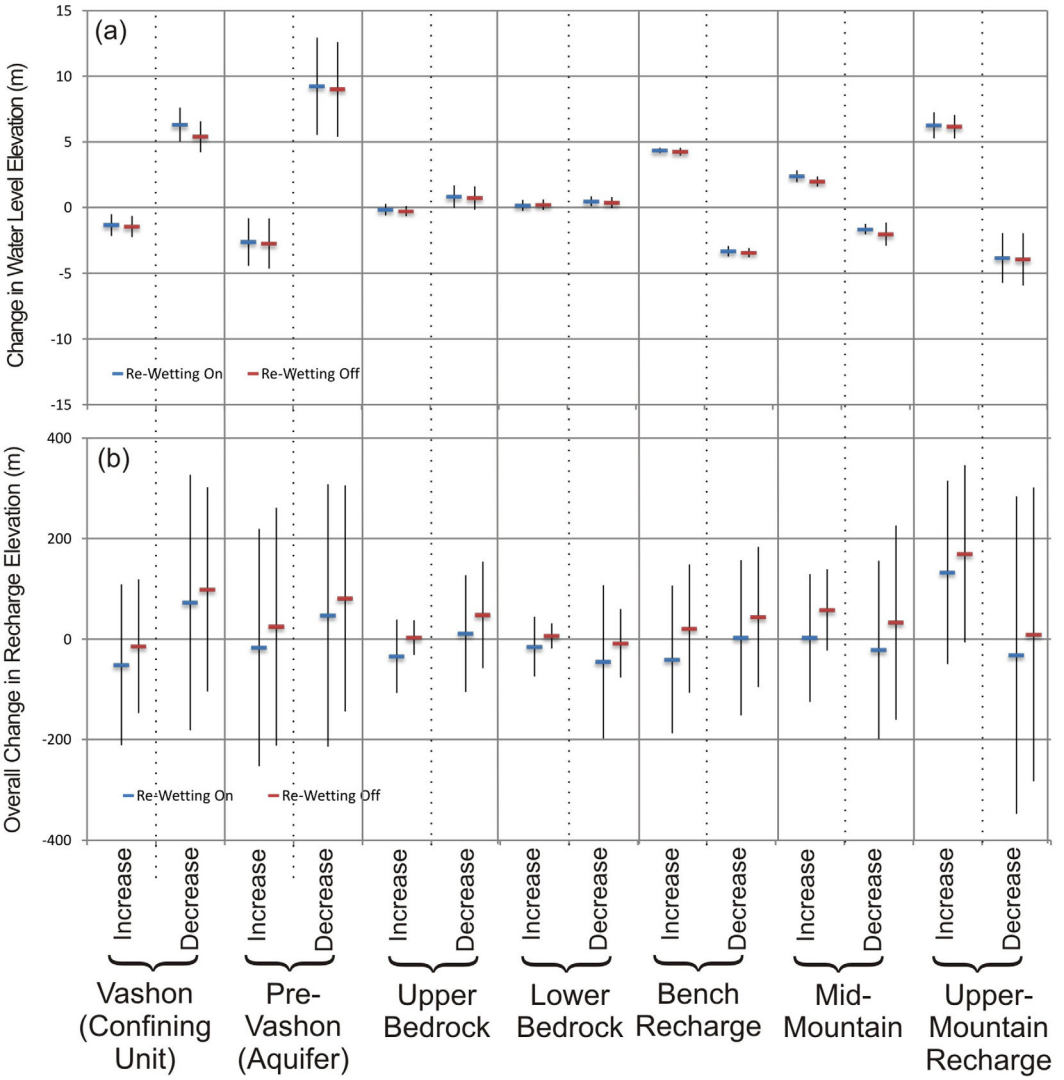

Figure 8. Overall model sensitivity plots for (a) water table elevation (hydraulic head) calculated by averaging the change in water levels in all of the wells and (b) recharge elevation calculated by averaging the change in mean elevation for all of the wells. Error bars on each data point are the standard deviation of the average change. For each variable, the change in head or recharge elevation is shown resulting from increasing and decreasing its value by 50%.

conductivity and recharge by ±50% to assess its influence on modeled heads and recharge elevation (Figures 8 and 9). Note that in the calibration process, K values were varied by a much larger amount (orders of magnitude). All analyses were initially run with rewetting activated; however, some did not converge given the parameter adjusted. As a result, the best fit model was run with both rewetting on and off and all sensitivity scenarios were compared to both cases. Overall, rewetting had a negligible effect on the sensitivity results.

The overall sensitivity of the water level elevation, calculated by averaging the change in water levels in all of the wells, is shown in Figure 8a. Figure 8b shows the overall sensitivity of recharge elevation determined by averaging the change in mean elevation for all of the wells. Error bars represent the standard deviation from the average change. Results show recharge elevation is sensitive to K and to the distribution and rates of recharge. Thus, recharge elevation is valuable for providing additional constraints on K as well as the location and rate of recharge. Second, recharge elevation is more sensitive to bedrock K than water levels are for a well network like this one lacking wells in the mountain block and in the bedrock underlying the bench, a common scenario in basin-fill aquifers in mountainous terrain. Finally, the sensitivity of recharge

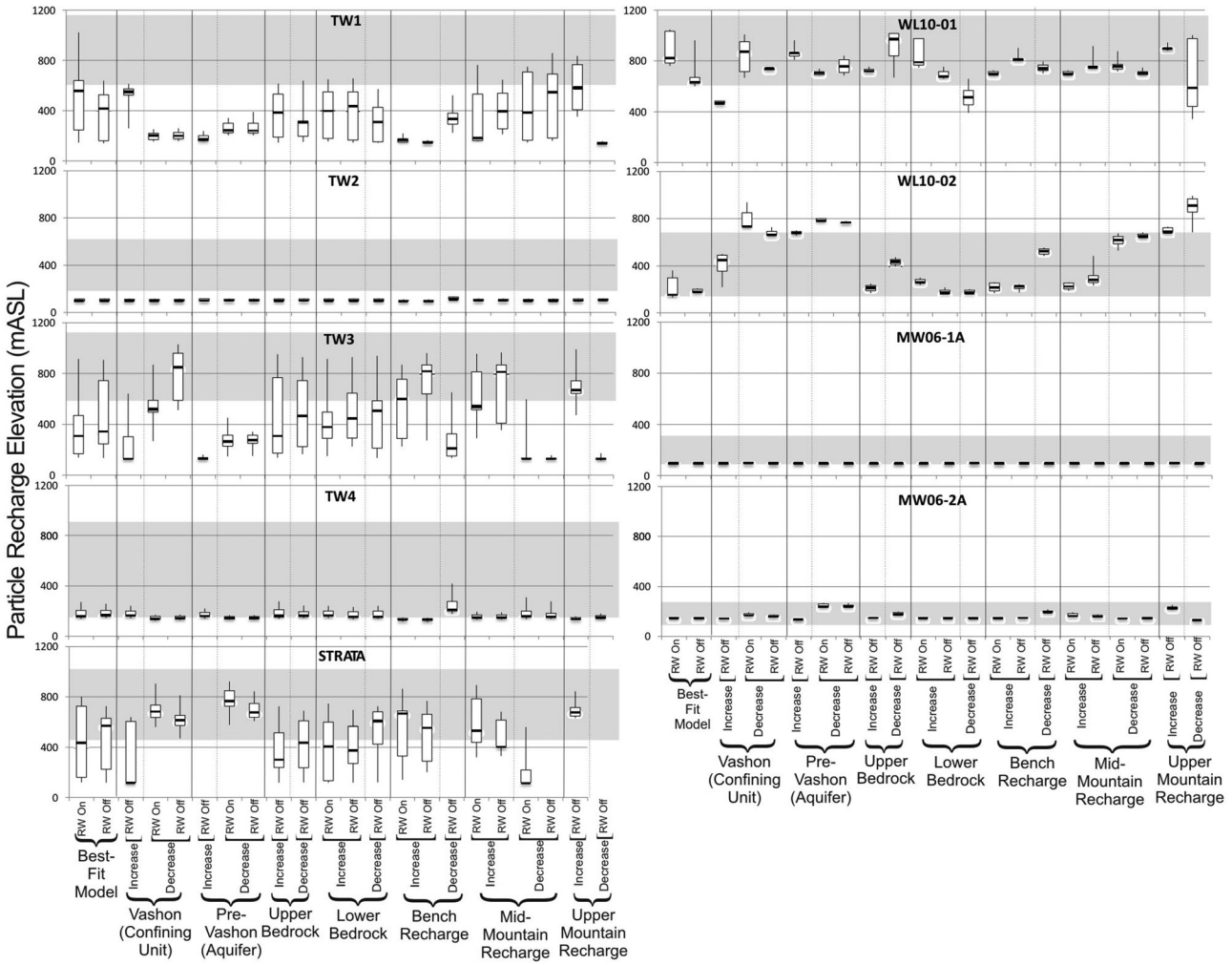

Figure 9. Comparision of measured and modeled recharge elevation ranges for best fit model. The variation of modeled recharge elevation with varying values of hydraulic conductivity and recharge rates is also shown. Box and stem symbols represent the range (and mean) of modeled recharge elevations based on the 10 backward-tracking particles released from each well screen. The shaded gray region signifies the range of the mean recharge elevation estimated from the noble gas data. For each variable, the modeled recharge elevation range resulting from increasing and decreasing its value by 50% is shown. RW indicates rewetting function.

elevation to all parameters is more variable well-to-well than the sensitivity of water levels. This means that increasing the number of bench wells in the observation network would likely produce little additional constraint if only water level data were collected from these (a case of diminishing returns). However, adding more wells if one is collecting noble gas data (recharge elevations) may provide substantial additional constraints, particularly if these wells are strategically located. It should be noted that the apparent sensitivity of heads to changes in the three recharge components (bench, midmountain, and upper mountain) is actually a sensitivity to total recharge rate rather than the distribution of recharge amongst the three areas (see section 4.5).

To exemplify the importance that recharge elevation has on constraining hydraulic parameters, recharge elevation box plots in Figure 9 explore the sensitivity of recharge elevation to K and to recharge rates and distribution for individual wells. Scenarios that could be run with cell rewetting on (RW On) were also run with cell rewetting off (RW Off) to compare the effect that rewetting has on the particle's recharge elevation. Recharge elevation was plotted for rewetting turned off only for scenarios that could not converge with rewetting turned on.

Recharge elevations in TW2, TW4, MW06-1A, and MW06-2A are relatively insensitive to any change of parameter value. These wells have the shallowest well screens, the lowest recharge elevation, and based on

environmental tracer results, the least amount of mountain block recharge water. As a result, flow paths are relatively short and are not affected by changes in upstream parameters.

TW1, TW3, and the Strata well show the greatest variance in recharge elevation. These wells are pumped regularly and environmental tracer results suggest that water from these wells is a mixture of mountain block recharge and bench recharge. The wide variance in particle recharge elevation likely represents a mixture of flow paths to each well.

Modeled recharge elevations in WL10-01 and WL10-02 are sensitive to all adjusted parameters. WL10-01 is located closest to the base of Mt. Elphinstone, has a very deep well screen, and tracer data suggest that most water flowing through the well is sourced from mountain block recharge. Recharge elevation appears to be most sensitive to increased K of the Vashon till zone, decreased K of the lower bedrock zone, and decreased recharge along the upper mountain. Increased conductivity of the Vashon till zone would create more recharge along the bench and therefore lower recharge elevations. This would result in a lower amount of mountain block recharge to the aquifer. Decreased K of the lower bedrock unit would also lower recharge elevations by preventing deep infiltration of groundwater that originates high up the mountain.

WL10-02 is located about half-way between the base of Mt. Elphinstone and the coastline. The well screen is also about middepth between the top of the water table and the base of the aquifer. Tracer results suggest that water flowing through WL10-02 could either be water recharged at midelevation, or a mixture of mountain block and bench recharged water. All box plots have a small range in recharge elevation suggesting that particles to WL10-02 recharge at midelevation. Backward-tracking particles are sensitive to the K of the Pre-Vashon and Vashon till zones, and to recharge rates in the midmountain and upper-mountain zones. In some cases, the increase or decrease in these parameters caused modeled mean recharge elevations to plot outside of the estimated recharge elevation range. The sensitivity of recharge elevation for wells WL10-01 and WL10-02 to K and the recharge distribution illustrates the value of recharge elevation estimates obtained from these locations in the aquifer for constraining K and recharge.

An additional sensitivity analysis was conducted in order to assess the effect that bedrock geometry has on hydraulic heads and recharge elevation. Six models were generated where specific areas within the upper and/or lower bedrock conductivity zones were changed to zones of Pre-Vashon or Vashon till in order to simulate changes in bedrock geometry. Modifications were performed in areas where no or limited bedrock data exists, such as borehole, well logs, geophysical profiles, or bedrock outcrops. The effect that changes in bedrock geometry have on recharge elevation is summarized in Figure 10. The plots show that backward-tracking particle recharge elevations are sensitive to bedrock geometry and that sensitivity varies with the location of bedrock altered.

Sensitivity of hydraulic heads (water table elevation) to bedrock geometry was also assessed and it was found that the water table elevation is relatively insensitive to each altered bedrock scenario. Calibration statistics for modeled versus observed heads for each scenario showed that only two out of the six scenarios had a maximum residual of greater than 2 m difference than the observed head. All but one scenario had correlation coefficients greater than 0.99 and all scenarios had acceptable normalized residual mean squares. Without the additional recharge elevation calibration targets to constrain bedrock geometry, at least four of the six altered bedrock scenarios could have been selected as the final model. Thus, these findings confirm the importance of having recharge elevation as an additional calibration target for minimizing model nonuniqueness. Although this could suggest that a number of these scenarios could produce a decent match to water level and recharge elevation by tweaking other parameters in the model, final K, and recharge parameters in the best fit model best represents our understanding of the current hydrogeological model based on all available geological, hydrogeological, and geochemical data.

These results exemplify the significance that recharge elevation has on constraining hydraulic parameters and provide calibration data where no physical data exists, especially in the mountain block where there is no other data to calibrate to.

4.5. Importance of Recharge Elevations Derived From Noble Gases

Prior to this study, recharge locations and processes were uncertain at this site and the contribution of mountain block recharge was considered negligible. To determine the value of the noble-gas-derived recharge elevations for constraining mountain block recharge, an additional numerical groundwater model

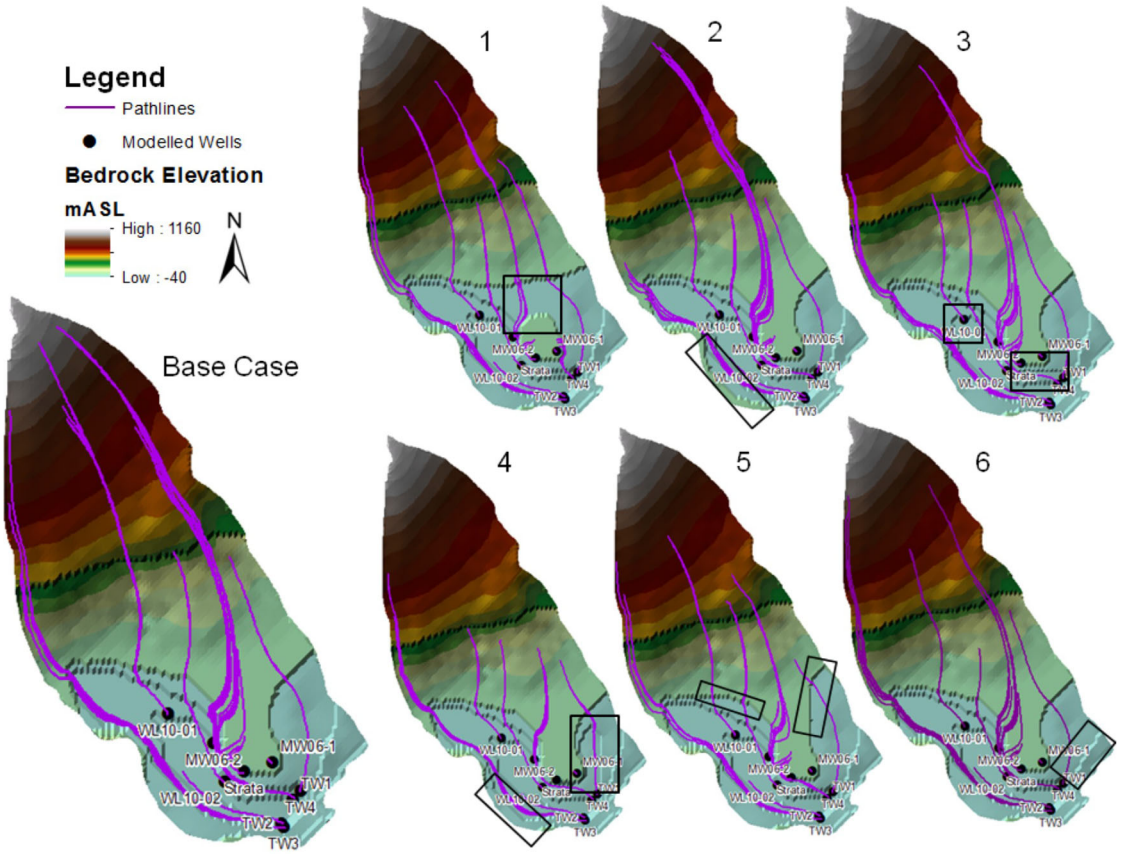

Figure 10. The effects that changes in bedrock geometry have on recharge elevation based on the backward-tracking particles released along each well's screen. Bedrock elevations grids were exported from Visual MODFLOW and regenerated in ArcGIS. Each model shows the change in recharge elevation, indicated by the endpoints of the purple path lines. The black boxes indicate areas where the bedrock surface was altered and is described as follows: (1) bedrock was removed from the base of the mountain to the bedrock knob; (2) a bedrock high was added to the southwest edge of the model; (3) the bedrock valley around WL10-01 was widened and bedrock was deepened in front of the knob between Strata and TW4/TW1; (4) a slight bedrock high was added to the southwest edge and the bedrock valley was deepened east of MW06-1; (5) the bedrock high was narrowed connecting the knob to the base of the mountain; and (6) bedrock was removed along the southeast edge of the model.

was constructed ("bench model") based on a conceptual model that excludes the mountain block and assumes no mountain block recharge. To do this, the original MODFLOW model was regenerated excluding the mountain block—the upper mountain zone shown in pink in Figure 11a.

Recharge rates were the only parameter adjusted in the bench model. All other model parameters were fixed and set equal to the best fit version of the original model. Boundary conditions also remained the same, but the lateral boundary where the mountain block was removed became a no-flow boundary. The bench model was calibrated to observed hydraulic heads only, and a similar close match between measured and modeled heads was achieved.

In the calibrated bench model, the recharge rate along the bench is nearly equal to that in the best fit version of the original model. However, the recharge rate in the midmountain zone along the base of Mt. Elphinstone is dramatically larger— 430 mm/yr compared to 130 mm/yr in the original model. Figure 11 shows the differences between the two models in daily recharge rates and the percentage of total recharge contributed by each recharge zone. In both models, the component of recharge through the bench is 35–36%. However, in the bench model, 64% of recharge occurs as infiltration through the Vashon till and Capilano glaciofluvial deposits at the base of Mt. Elphinstone compared to 19% in the original model. The percentage of midmountain zone precipitation that becomes recharge in the bench model is relatively high (30%), but still entirely plausible. This exercise clearly demonstrates that hydraulic head data alone are incapable of quantifying mountain block recharge. In the absence of the noble gas data, it is likely that the same recharge assumptions would have been made as in previous studies [*Piteau Associates Engineering Ltd*, 2006; *Waterline Resources Inc*., 2010] and the contribution of mountain block recharge would have been

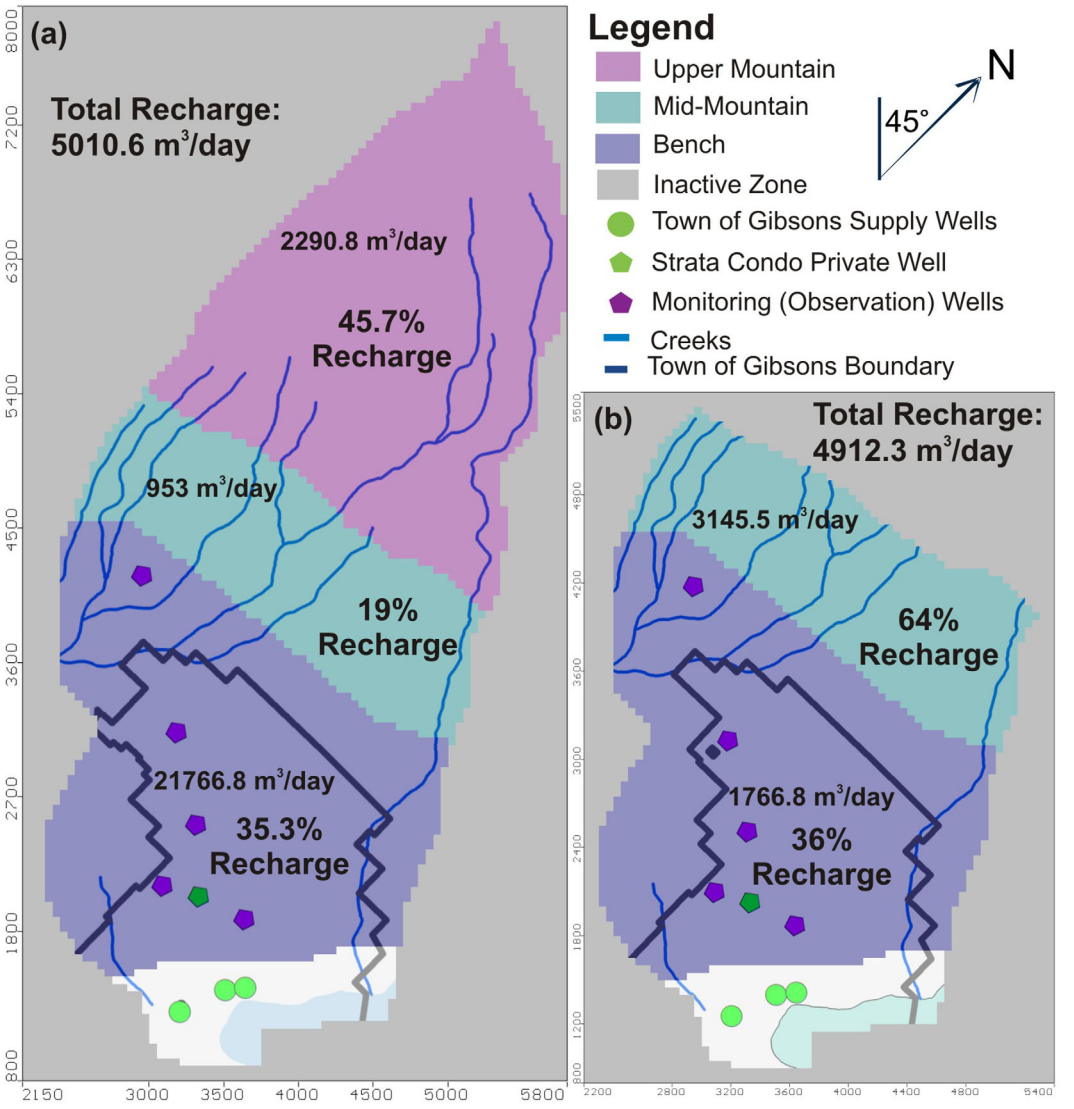

Figure 11. Comparison of recharge components in daily total recharge rates and the percent of total recharge for each recharge zone for (a) the original model and (b) the no mountain block recharge model.

overlooked. Insights from environmental tracers significantly improved the understanding of recharge to the Gibsons aquifer.

5. Conclusions

This study exemplifies the value of using noble gases as environmental tracers to improve the understanding of the conceptual model and to effectively constrain and calibrate a groundwater flow model of the Gibsons aquifer. The distribution of apparent $^{3}H/^{3}He$ ages and noble gas calculated recharge temperatures improved the current understanding of the conceptual hydrogeological model by identifying two components of recharge to the Gibsons aquifer: (1) modern water (<10 years old) with warm recharge temperatures (~9°C) that recharges at low elevations by leakage through the Vashon till and (2) premodern water (>60 years old) with cold recharge temperatures (5–6°C) that recharges and flows through fractures in bedrock along Mt. Elphinstone and into the Gibsons aquifer as mountain block recharge.

The updated conceptual model was integrated into a three-dimensional numerical groundwater flow model that was calibrated to hydraulic heads and to recharge elevations estimated using noble gas recharge temperatures. Recharge elevations were imperative in constraining hydraulic parameters and bedrock

geometry which minimized model nonuniqueness in cases where hydraulic heads were insensitive. Modeling results indicate that 45% of recharge to the Gibsons aquifer is from mountain block recharge which translates to 8% of the total annual precipitation over the mountain.

This study also demonstrates that hydraulic head data from a low-elevation aquifer alone are incapable of quantifying mountain block recharge. Acceptable calibration to hydraulic head data was also achieved using a numerical model that excludes the mountain block and includes no mountain block recharge. Results of this study have significant implications for understanding and managing source water protection in recharge areas, potential effects of climate change, the overall water budget, and ultimately ensuring groundwater sustainability.

Acknowledgments
Data are either reported in section 4 or available from http://circle.ubc.ca/handle/2429/45015. The authors would like to thank our collaborative partners Waterline Resources, the Town of Gibsons and Gordon Groundwater Consultancy. This research was supported by a Natural Sciences and Engineering Research Council of Canada and Waterline Resources. We would also like to thank Kip Solomon and Alan Rigby for laboratory analysis as well as the Associate Editor Olaf Cirpka, Werner Aeschbach-Hertig, and one anonymous reviewer for greatly improving the manuscript.

References

Aeschbach-Hertig, W., F. Peeters, U. Beyerle, and R. Kipfer (1999), Interpretation of dissolved atmospheric noble gases in natural waters, *Water Resour. Res.*, *35*, 2779–2792.

Aeschbach-Hertig, W., F. Peeters, U. Beyerle, and R. Kipfer (2000), Palaeotemperature reconstruction from noble gases in ground water taking into account equilibration with entrapped air, *Nature*, *405*(6790), 1040–1044.

Ajami, H., P. A. Troch, T. Maddock III, T. Meixner, and C. Eastoe (2011), Quantifying mountain block recharge by means of catchment-scale storage-discharge relationships, *Water Resour. Res.*, *47*, W04504, doi:10.1029/2010WR009598.

Anderman, E. R., M. C. Hill, and E. P. Poeter (1996), Two-dimensional advective transport in ground-water flow parameter estimation, *Ground Water*, *34*(6), 1001–1009.

Anderson, M. P. (2005), Heat as a ground water tracer, *Ground Water*, *43*, 951–968.

Anderson, T. W., G. W. Freethy, and P. Tucci (1992), Geohydrology and water resources of alluvial basins in south central Arizona and parts of adjacent states, *U.S. Geol. Surv. Prof. Pap., 1406-B*, pp. B1–B67.

Armstrong, J. E. (1981), Post-Vashon Wisconsin glaciation, Fraser Lowland British Columbia, *Bull. Geol. Surv. Can.*, *322*, 34 pp.

Ballentine, C. J., and C. M. Hall (1999), An inverse technique for calculating paleotemperatures and other variables using noble gas concentrations in groundwater, *Geochim. Cosmochim. Acta*, *63*, 2315–2336.

Bayer, R., P. Schlosser, G. Bonisch, H. Rupp, F. Zaucker, and G. Zimmek (1989), Performance and blank components of a mass spectrometric system for routine measurement of helium isotopes and tritium by the ^{3}He ingrowth method, in *Sitzungsberichte der Heidelberger Akademie der Wissenchaften, Mathematisch-Naturwissenschaftliche Klasse*, vol. 5, edited by Heidelberg Academy of Sciences, pp. 241–279, Springer, N. Y.

Beyerle, U., W. Aeschbach-Hertig, M. Hofer, D. M. Imboden, H. Baur, and R. Kipfer (1999), Infiltration of river water to a shallow aquifer investigated with ^{3}H/^{3}He, noble gases and CFCs, *J. Hydrol.*, *220*(3–4), 169–185.

Chavez, A., S. N. Davis, and S. Sorooshian (1994a), Estimation of mountain-front recharge to regional aquifers 1: Development of an analytical hydroclimatic model, *Water Resour. Res.*, *30*, 2157–2167.

Chavez, A., S. Sorooshian, and S. N. Davis (1994b), Estimation of mountain-front recharge to regional aquifers 2: A maximum likelihood approach incorporation prior information, *Water Resour. Res.*, *30*, 2169–2181.

Christensen, H., M. C. Hill, D. Rosbjerg, and K. H. Jensen (1995), Three-dimensional inverse modeling using heads and concentration at a Danish landfill, in *Proceedings of IAHS-IUGG XXI General Assembly*, edited by B. Wagner and T. Illangesekare, *IAHS Publ., 27*, pp. 167–175.

Clague, J. J. (1977), Quadra sand: A study of the Late Pleistocene geology and geomorphic history of Coastal Southwest British Columbia, *Geol. Surv. Can. Pap., 77–17*, 24 pp.

Clarke, W. B., W. J. Jenkins, and Z. Top (1976), Determination of tritium by mass spectrometric measurements of ^{3}He, *Int. J. Appl. Radiat. Isot.*, *27*, 515–522.

Cook, P. G., and J. Bohlke (2000), Determining timescales for groundwater flow and solute transport, *Environmental Tracers in Subsurface Hydrology*, edited by P. Cook and A. L. Herczeg, 1–30 pp., Kluwer Acad.

Cook, P. G., A. J. Love, N. I. Robinson, and C. T. Simmons (2005), Groundwater ages in fractured rock aquifers, *J. Hydrol.*, *308*, 284–301.

Doyle, J. M. (2013), Integrating environmental tracers and groundwater flow modeling to investigate groundwater sustainability, MSc thesis, 183 pp., Univ. of British Columbia, Gibsons, B. C.

Environment Canada (2012), Gower point climate station data record from 1971–2000, Fredericton, New Brunswick. [Available at http://www.climate.weatheroffice.gc.ca/climate_normals/station_metadata_e.html?StnId=309.]

Forster, C. B., and L. Smith (1988), Groundwater flow systems in mountainous terrain: 2. Controlling factors, *Water Resour. Res.*, *24*, 1011–1023.

Friedman, R. M., J. W. H. Monger, and H. W. Tipper (1990), Age of the Bowen Island Group, southwestern Coast Mountains, British Columbia, *Can. J. Earth Sci.*, *27*(11), 1456–1461.

Fyles, J. G. (1963), Surficial geology of Horne Lake and Parksville map-areas, Vancouver Island, British Columbia, *Mem. Geol. Surv. Can. 318*, 142 pp.

Gannett, M. W., K. E. Lite, D. S. Morgan, and C. A. Collins (2001), Ground-water hydrology of the Upper Deschutes Basin, Oregon, *U.S. Geol. Surv. Water Resour. Invest. Rep., 00-4162*, 77 pp.

Gardner, P., and D. K. Solomon (2009), An advanced passive diffusion sampler for the determination of dissolved gas concentrations, *Water Resour. Res.*, *45*, W06423, doi:10.1029/2008WR007399.

Gleeson, T., and A. H. Manning (2008), Regional groundwater flow in mountainous terrain: Three-dimensional simulations of topographic and hydrogeologic controls, *Water Resour. Res.*, *44*, W10403, doi:10.1029/2008WR006848.

Gleeson, T., J. VanderSteen, M. A. Sophpcleous, M. Taniguchi, W. M. Alley, D. M. Allen, and Y. Zhou (2010), Groundwater sustainability strategies, *Nat. Geosci.*, *3*, 378–379.

Goode, D. J. (1996), Direct simulation of groundwater age, *Water Resour. Res.*, *32*, 289–296.

Heilweil, V. M., R. W. Healy, and R. N. Harris (2012), Noble gases and coupled heat/fluid flow modeling for evaluating hydrogeologic conditions of volcanic island aquifers, *J. Hydrol.*, *164–164*, 309–327.

Kahn, K. G., G. Shemin, J. S. Caine, and A. Manning (2008), Characterization of the shallow groundwater system in an alpine watershed: Handcart Gulch, Colorado, USA, *Hydrogeol. J.*, *16*(1), 103–121.

Magruder, I. A., W. W. Woessner, and S. W. Running (2009), Ecohydrologic-process modeling of mountain-block ground water recharge, *Ground Water*, *47*(6), 774–785.
Manning, A. H. (2011), Mountain-block recharge, present and past, in the eastern Española Basin, New Mexico, USA, *Hydrogeol. J.*, *19*(2), 379–397.
Manning, A. H., and J. S. Caine (2007), Groundwater noble gas, age, and temperature signatures in an Alpine watershed: Valuable tools in conceptual model development, *Water Resour. Res.*, *43*, W04404, doi:10.1029/2006WR005349.
Manning, A. H., and D. K. Solomon (2003), Using noble gases to investigate mountain-front recharge, *J. Hydrol.*, *275*(3–4), 194–207.
Manning, A. H., and D. K. Solomon (2005), An integrated environmental tracer approach to characterizing groundwater circulation in a mountain block, *Water Resour. Res.*, *41*, W12412, doi:10.1029/2005WR004178.
Masbruch, M. D., D. S. Chapman, and D. K. Solomon (2012), Air, ground, and groundwater recharge temperatures in an alpine setting, Brighton Basin, Utah, *Water Resour. Res.*, *48*, W10530, doi:10.1029/2012WR012100.
Monger, J. W. H. (1994), Introduction, in *Geology and Geological Hazards of the Vancouver Region, Southwestern British Columbia*, edited by J. W. H. Monger, *Bull. Geol. Surv. Can. 481*, pp. 1–2.
Monger, J. W. H., and J. M. Journeay (1994), Basement geology and tectonic evolution of the Vancouver region, in *Geology and Geological Hazards of the Vancouver Region, Southwestern British Columbia*, edited by J. W. H. Monger, *Bull. Geol. Surv. Can., 481*, pp. 3–25.
Newman, B. D., K. Osenbruck, W. Aeschbach-Hertig, D. K. Solomon, P. Cook, K. Rozanski, and R. Kipfer (2010), Dating of young groundwaters using environmental tracers: Advantages, applications, and research needs, *Isot. Environ. Health Stud.*, *46*(3), 259–278.
Piteau Associates Engineering Ltd. (2006), *Well Head Protection Assessment for Gibsons, B. C., Final Draft, Project 2539*, 23 pp, North Vancouver, B. C.
Plummer, L. N. (2005), Dating of young groundwater, in *Isotopes in the Water Cycle: Present and Future of a Developing Science*, edited by P. K. Aggarwal, J. R. Gat, and K. F. O. Froehlich, pp. 193–218, Springer, Netherlands.
Reilly, T. E., and A. W. Harbaugh (2004), Guidelines for evaluating ground-water flow models, *U.S. Geol. Surv. Sci. Invest. Rep., 2004-5038*, 30 pp., U.S. Dep. of the Int., U.S. Geol. Surv.
Reilly, T. E., L. N. Plummer, P. J. Phillips, and E. Busenberg (1994), The use of simulation and multiple environmental tracers to quantify groundwater flow in a shallow aquifer, *Water Resour. Res.*, *30*, 421–433.
Sanford, W. (2002), Recharge and groundwater models: An overview, *Hydrogeol. J.*, *10*, 110–120.
Sanford, W. (2011), Calibration of models using groundwater age, *Hydrogeol. J.*, *19*, 13–16.
Sanford, W. E., L. N. Plummer, D. P. McAda, L. M. Bexfield, and S. K. Anderholm (2004), Hydrochemical tracers in the middle Rio Grande Basin, USA: 2. Calibration of a groundwater-flow model, *Hydrogeol. J.*, *12*(4), 389–407.
Scanlon, B. R., W. H. Healy, and P. G. Cook (2002), Choosing appropriate techniques for quantifying groundwater recharge, *Hydrogeol. J.*, *10*, 18–39.
Schlosser, P., M. Stute, H. Dörr, C. Sonntag, and K. O. Münnich (1988), Tritium/^{3}He dating of shallow groundwater, *Earth Planet. Sci. Lett.*, *89*(3/4), 353–362.
Schlosser, P., M. Stute, C. Sonntag, and C. O. Munnich (1989), Tritogenic ^{3}He in shallow groundwater, *Earth Planet. Sci. Lett.*, *94L*, 245–256.
Senthilkumar, M., and L. Elango (2004), Three-dimensional mathematical model to simulate groundwater flow in the lower Palar River basin, southern India, *Hydrogeol. J.*, *12*(2), 197–208.
Smerdon, B. D., D. M. Allen, S. E. Grasby, and M. A. Berg (2009), An approach for predicting groundwater recharge in mountainous watersheds, *J. Hydrol.*, *365*(3–4), 156–172.
Solomon, D. K., and P. G. Cook (2000), ^{3}H and ^{3}He, in *Environmental Tracers in Subsurface Hydrology*, edited by P. Cook and A. L. Herczeg, pp. 397–424, Kluwer Acad, Netherlands.
Statistics Canada (2011), Town of Gibsons census profile (2011), Gov. of Can, Ottawa, Ont. [Available at http://www12.statcan.gc.ca/census-recensement/2011/dp-pd/prof/index.cfm?Lang=E.]
Stute, M., and P. Schlosser (1993), Principles and applications of the noble gas paleothermometer, in *Climate Change in Continental Isotope Records*, edited by P. K. Swart et al., pp. 89–100, AGU, Washington, D. C.
Waterline Resources Inc. (2010), *Interim Report: Aquifer Mapping Study*, 45 p., Town of Gibsons, B. C.
Welch, L. A., and D. M. Allen (2012), Consistency of groundwater flow patterns in mountainous topography: Implications for valley bottom water replenishment and for defining groundwater flow boundaries, *Water Resour. Res.*, *48*, W05526, doi:10.1029/2011WR010901.
Welch, L. A., and D. M. Allen (2014), Hydraulic conductivity characteristics in mountains and implications for conceptualizing bedrock groundwater flow, *Hydrogeol. J.*, *22*, 1003–1026.
Wilson, J. L., and H. Guan (2004), Mountain-block hydrology and mountain-front recharge, in *Groundwater Recharge in a Desert Environment: The Southwestern United States*, edited by J. F. Hogan, F. M. Phillips, and B. R. Scanlon, pp. 113–137, AGU, Washington, D. C.